



## Dimming/brightening over the Iberian Peninsula: Trends in sunshine duration and cloud cover and their relations with atmospheric circulation

Arturo Sanchez-Lorenzo,<sup>1</sup> Josep Calbó,<sup>2</sup> Michele Brunetti,<sup>3</sup> and Clara Deser<sup>4</sup>

Received 31 October 2008; revised 7 February 2009; accepted 18 February 2009; published 24 April 2009.

[1] This study analyzes the spatial and temporal changes in sunshine duration (SunDu) and total cloud cover (TCC) over the Iberian Peninsula (IP) and four subregions during 1961–2004 using high-quality, homogenized data sets. The analyses confirm that over most of the IP and in most seasons, SunDu and TCC variations are strongly negatively correlated, with absolute values  $\sim 0.8$ – $0.9$ . Somewhat weaker correlations ( $0.5$ – $0.6$ ) are found in the southern portion of the IP in summer. A large discrepancy between the SunDu and TCC records occurs from the 1960s until the early 1980s when the SunDu series shows a decrease that it is not associated with an increase in TCC. This negative trend or “dimming” is even more pronounced after removing the effects of TCC via linear regression. Since the early 1980s, the SunDu and TCC residual SunDu series exhibit an upward trend or “brightening.” In addition to the long-term dimming and brightening, the volcanic eruptions of El Chichon and Mount Pinatubo are clearly evident in the TCC residual SunDu record. The TCC and SunDu records over the IP are well correlated with sea level pressure (SLP), with above normal TCC and below normal SunDu corresponding to below normal SLP locally in all seasons. The TCC and SunDu related SLP changes over the IP in winter and spring are part of a larger-scale north-south dipole pattern that extends over the entire Euro-Atlantic sector. Other more regional atmospheric circulation patterns, identified from rotated principal component analysis, are also linked to TCC and SunDu variations over the IP. Finally and perhaps surprisingly, the TCC residual SunDu series exhibits a statistically significant relationship with a regional atmospheric circulation pattern during spring, summer, and autumn.

**Citation:** Sanchez-Lorenzo, A., J. Calbó, M. Brunetti, and C. Deser (2009), Dimming/brightening over the Iberian Peninsula: Trends in sunshine duration and cloud cover and their relations with atmospheric circulation, *J. Geophys. Res.*, *114*, D00D09, doi:10.1029/2008JD011394.

### 1. Introduction

[2] Within the last few decades, considerable changes in the physical climate system have been detected globally. Many of these changes have been attributed, with a very high confidence level, to anthropogenic influences [Solomon *et al.*, 2007]. The most studied variable, global mean near-surface air temperature, has risen by  $0.74 \pm 0.18^\circ\text{C}$  over the last century (1906–2005), with a rate of warming over the last 50 years ( $0.13 \pm 0.03^\circ\text{C}$  per decade) that is nearly twice that for the last 100 years and has no precedents in the instrumental records [Trenberth *et al.*, 2007]. Therefore, global warming is a phenomenon established with high confidence, while other climate variables bring more uncer-

tainties regarding their changes and responses to anthropogenic forcing. For example, there are still large uncertainties about how clouds will respond to climate change, despite important advances in understanding during recent years. Consequently, cloud feedbacks are the primary source of intermodel differences in equilibrium climate sensitivity, with low clouds being the largest contributor [Solomon *et al.*, 2007].

[3] Clouds are the main cause of interannual and decadal variability of radiation reaching the Earth’s surface and therefore they exert a dominant influence on the global energy balance. In fact, cloudiness can contribute to cooling, i.e., low-level clouds types linked to their high albedo [Mace *et al.*, 2006], but also to warming, i.e., high clouds types emit less radiation out to space than do low clouds or the clear atmosphere [Lynch, 1996; Mace *et al.*, 2006]. Regarding climatic studies of cloudiness, a distinction must be made between studies based on ground level visual observations and studies based on satellite data. A discussion about the advantages and limitations of both sources of data are given by Warren and Hahn [2002]. Although an accurate assessment of cloudiness variations on global or hemispheric scales

<sup>1</sup>Group of Climatology, Department of Physical Geography, University of Barcelona, Barcelona, Spain.

<sup>2</sup>Group of Environmental Physics, University of Girona, Girona, Spain.

<sup>3</sup>Institute of Atmospheric Sciences and Climate, Italian National Research Council (ISAC-CNR), Bologna, Italy.

<sup>4</sup>National Center for Atmospheric Research, Boulder, Colorado, USA.

can only be obtained through the use of satellite images, climate analyses of such images is limited by the short period of available data and also by calibration issues that undermine construction of homogeneous data sets required for detecting climatic long-term trends.

[4] On the other hand, a widespread reduction of global solar radiation between the 1950s and 1980s has been well established and documented [e.g., *Ohmura and Lang, 1989; Gilgen et al., 1998; Stanhill and Cohen, 2001; Liepert, 2002*], and since late 1980s a reversal in this trend has been detected in many regions of the world [*Pinker et al., 2005; Wild et al., 2005*]. This decrease and increase in surface solar radiation have been defined as “global dimming” and “global brightening,” respectively. Although causes of this phenomenon are not fully understood currently, changes in the transmissivity of the Earth’s atmosphere due to changes in concentrations and optical properties of aerosols as consequence of anthropogenic emissions are considered the most likely causes [*Stanhill and Cohen, 2001; Wild et al., 2005, 2007*].

[5] However, both the global dimming and the recent brightening carry uncertainty in their explanation and quantification as recently remarked the IPCC Fourth Assessment Report [*Trenberth et al., 2007, p. 279*]. For example, some studies found that the dimming period appears more clearly in large urban areas as a consequence of local pollution and consequently it might not be a global phenomenon [*Alpert et al., 2005; Alpert and Kishcha, 2008*]. These studies also pointed out the lack of stations with reliable and long-term series of global radiation measurements in rural areas and in nondeveloped countries. Since cloudiness is the largest modulator of solar radiation reaching the ground, it has also been suggested that the dimming period may be linked to a detected increase in total cloud cover since the second half of the 20th century over many regions in the world [*Dai et al., 1999*]. This increasing cloudiness since 1950 is consistent with an increase in precipitation and a decrease in daily temperature range [*Vose et al., 2005*]. In contrast, a decrease in total cloud cover over land, from visual observations and remote sensing [*Rossow and Dueñas, 2004; Warren et al., 2007*], has been reported since the late 1970s or the early 1980s; this cloudiness change can be reasonably related to the brightening period [*Wild et al., 2005*].

[6] However, it must be noted that during the dimming period there were areas with decreasing cloudiness [e.g., *Kaiser, 2000; Maugeri et al., 2001; Auer et al., 2007*], and also areas lacking cloud cover trends but decreases in solar radiation reaching the surface [e.g., *Stanhill and Moreshet, 1992; Stanhill and Cohen, 2001; Qian et al., 2006*]. Also, different studies have detected changes in global solar radiation under clear skies [*Abakumova et al., 1996; Wild et al., 2005; Ruckstuhl et al., 2008*] and cloudy skies [*Liepert, 2002*], presumably due to variations in atmospheric transparency linked to changes in anthropogenic aerosols. Recent changes in emissions of the main anthropogenic aerosols have been reported [*Stern, 2006; Streets et al., 2006*] and may be partially responsible for the transition between the dimming and brightening periods. Besides the direct aerosol effect, i.e., aerosol capacity to scatter or absorb solar radiation, it is important to consider as well the aerosol indirect effects. These indirect effects are more uncertain

and correspond to aerosol induced changes in cloud properties such as lifetime and albedo, and have also been linked to modification of precipitation forming processes [e.g., *Ramanathan et al., 2001; Rosenfeld et al., 2008*]. In fact, since most IPCC climate models did not include the aerosol indirect effects, it has been suggested that the agreement between observed and simulated surface warming may be partly spurious [*Knutti, 2008*].

[7] A difficulty in establishing causes of the global dimming and brightening is the limited number of solar radiation series with accurate and calibrated long-term measurements. For this purpose, the analysis should be supported and extended with the use of other climatic variables such as evaporation, visibility, or sunshine duration (SunDu) records [*Stanhill, 2005*], especially with series starting before the 1950s or in regions where solar radiation measurements are not available. SunDu is defined as the amount of time, usually expressed in number of hours, that direct solar radiation exceeds a certain threshold (usually taken at  $120 \text{ W m}^{-2}$ ). Consequently, this variable can be considered as an excellent proxy measure of global solar radiation on interannual [e.g., *Iqbal, 1983; Stanhill, 2003*] and also on decadal scales [e.g., *Liang and Xia, 2005; Stanhill and Cohen, 2008*], playing an important role in the description of global dimming and brightening phenomena.

[8] Moreover, an interesting way of investigating possible explanations of interannual and decadal variability of radiation, SunDu, and/or cloudiness consists in analyzing their relationships to the atmospheric circulation patterns or “teleconnections,” that normally are summarized by indices that simplify the spatial structure of pressure systems and that can be used as time series showing the evolution in amplitude and phase of these modes of atmospheric variability [*Hurrell et al., 2003; Trenberth et al., 2007*]. Many circulation patterns or teleconnections have been identified for the Northern Hemisphere that normally tend to be most prominent in winter, when the mean circulation is stronger [e.g., *Barnston and Livezey, 1987; Hurrell et al., 2003*]. Decadal variations in the persistence of these circulation patterns can be associated with regional changes in different climatic variables, and consequently during the last decades a growing interest has been put on circulation patterns changes that may be indirectly related to the recent climate change of anthropogenic origin [*Solomon et al., 2007*].

[9] The Iberian Peninsula (IP) is a region with few long-term solar radiation records [*Norris and Wild, 2007*]. However, a collection of 72 SunDu series over the IP has recently been compiled and homogenized by *Sanchez-Lorenzo et al.* [2007] (hereafter referred to as SL07). The resulting annual SunDu series for the whole IP confirms a period of dimming from the 1950s to the early 1980s, followed by a period of brightening until the end of the 20th century (SL07).

[10] In SL07, however, the role of cloudiness in SunDu variability was not explored, despite the fact that it is well known that both variables are inversely related [e.g., *Angell et al., 1984; Angell, 1990; Jones and Henderson-Sellers, 1992*]. Few studies on cloudiness climatology are published for the IP or Spain; a recent work compared total cloud cover (TCC) from different sources, and showed consistent declining trends for both reanalysis values (ERA-40) and remote sensing data (ISSCP) [*Calbó and Sanchez-Lorenzo, 2009*].

[11] Thus, the main objective of our study is to compare high-quality data sets of SunDu and TCC series over the IP, in order to determine the degree of agreement between both variables at different spatial and temporal resolutions, putting a special emphasis in detecting possible dimming/brightening subperiods over IP. The second objective is to determine the main atmospheric circulation patterns over the Euro-Atlantic sector linked with SunDu and TCC variations on interannual and decadal time scales. In section 2, we describe the SunDu and TCC data sets and methods used in this study. The annual and seasonal comparison of both variables is presented in section 3, and a residual SunDu series is defined by removing the linearly associated TCC variability. In section 4, the relationships between the TCC and SunDu series and prominent atmospheric circulation patterns are shown. Finally, conclusions of this paper are presented in section 5.

## 2. Data Sets and Methods

### 2.1. Sunshine Duration and Cloudiness Data Sets

[12] The SunDu data set used here is the same that was described and used in SL07, where details on the original data, quality control checks, homogenization procedure, and gridding method can be consulted. The final data set is a  $1^\circ$  (latitude and longitude) resolution gridded version that covers the whole IP with 84 cells and complete records from 1951 until 2004. For the present study we used the annual and seasonal series for the whole IP and 4 subregions obtained by means of a Principal Component Analysis (PCA).

[13] The original cloudiness series used in this study were obtained from the Spanish Agencia Estatal de Meteorología (AEMET) formerly named Instituto Nacional de Meteorología and also from the Portuguese Instituto de Meteorologia. The cloudiness database is constituted by 83 daily series of TCC measured consistently in oktas, obtained from the average of 3-daily observations taken at 7, 13 and 18 UTC; all series are at least 30 years long and end in December 2004. Since SunDu records integrate insolation during all daylight hours, these 3 cloudiness observations per day seem adequate to define a mean TCC that can be compared with SunDu series. Following the recommendations of *Aguilar et al.* [2003] we applied different quality control checks in order to (1) detect and correct/remove gross errors, such as aberrant (e.g., TCC values greater than 8 oktas) or negative values; (2) remove false zeros that can be an important source of error when estimating the monthly mean; and (3) check the consistency of calendar dates (days per year or month). Following these quality control checks, the daily series were converted into monthly values, by averaging the daily series of TCC in monthly mean values. When more than 6 days in a month were missing, we did not compute the monthly value, and the whole month was set as missing.

[14] After obtaining the monthly series, we tested the homogeneity of the TCC series. Note that these series can bring important inhomogeneities since are visual observations recorded by meteorological observers, so they are partially subjective. Although there are many examples of works that apply homogenization procedures to different climatic variables, such as temperatures or precipitation [e.g., see *Aguilar et al.*, 2003, and references therein], few studies have yet applied a homogeneity procedure on cloud-

iness series. *Maugeri et al.* [2001] and *Auer et al.* [2007] are some of the few exceptions: both works demonstrate that TCC series are affected by temporal breaks that must be corrected or eliminated before the assessment of long-term changes in cloudiness. In the present work, the Craddock relative homogeneity test [*Craddock*, 1979] was applied based in a modification detailed by *Brunetti et al.* [2006] and SL07. We rejected for the subsequent analyses 14 complete series with many inhomogeneities, and we also removed several subperiods of other series. Thus, the final monthly TCC data set consists of 69 series across the whole IP (Figure 1). Although there are some series with data starting in the 1930s, there is a clear increase of data availability only after 1961. Therefore, we limited the cloudiness and SunDu data sets to the 1961–2004 period.

[15] Then, all gaps between the first available year of each series and December 2004 were filled with estimates based upon the highest correlated reference (neighboring) series. Finally, we generated a gridded version for the TCC data sets in order to minimize possible errors resulting from eventually persistent inhomogeneities and to overcome problems related to nonhomogeneous spatial coverage of the stations. We followed the same interpolation technique described in SL07 and the grid was constructed for the same domain ( $9^\circ\text{W}$ – $3^\circ\text{E}$ ;  $36^\circ\text{N}$ – $45^\circ\text{N}$ ), at the same  $1^\circ$  spatial resolution (Figure 1), and was calculated at monthly, seasonal, and annual resolution, on the basis of single station anomaly series (obtained as ratio to the corresponding 1971–2000 mean). The reliability of these TCC gridded series was then confirmed by comparison with daily temperature range data [*Sanchez-Lorenzo et al.*, 2008b]. Thus, TCC grid can be easily compared with SunDu data set since both variables used a similar number of initial series and have been converted to the same grid domain and spatial resolution using the same interpolation gridding technique.

### 2.2. SunDu and TCC Regionalization and Mean Series Construction

[16] Since we decided to study the spatial behavior of differences between TCC and SunDu over the IP, we started by establishing different subregions in the area. As in SL07 for the SunDu series, for the TCC data set the regionalization approach was based on a S-Mode PCA [*Preisendorfer*, 1988] that defines the main modes of temporal variability in TCC over the IP. We applied the PCA to the gridded data set, starting from the correlation matrix, and considering all the 12 monthly anomalies of the year in order to obtain a unique regionalization and to avoid inconvenient seasonal differentiation. Six of the obtained Empirical Orthogonal Functions (EOF) have eigenvalues greater than 1, explaining together near the 94% of the total variance in the data set. Only the first four EOF, which have eigenvalues greater than 2, were retained and a Varimax rotation was applied to the corresponding eigenvector. The obtained regions are almost identical to those obtained with the SunDu series (SL07, Figure 5), and consequently we defined exactly the same 4 subregions in order to simplify the comparison between both variables. Summarizing the results, we identified 4 subregions which comprise the central-east (E), north (N), west (W) and southern (S) sectors of the IP. Subsequently, we computed the TCC annual and seasonal mean series for the whole IP and the 4 subregions as an arithmetic mean of

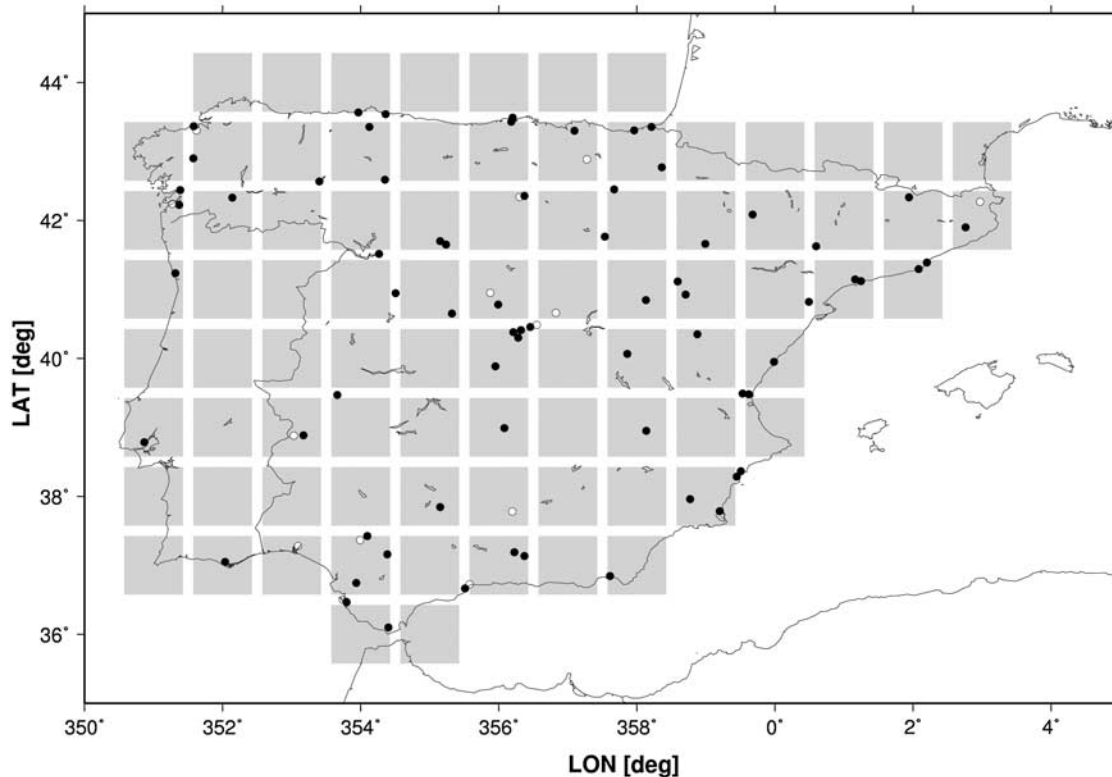


**Figure 1.** Location of the 83 cloudiness series obtained for the IP, with indication of the 69 selected (black circles) and 14 rejected (white circles) stations after the homogenization procedure. The 84 grid cells generated with  $1^\circ$  of spatial resolution are indicated too.

the 84 grid cells and of the corresponding grid cells in each subregion, respectively. This spatial averaging approach enhances the signal-to-noise ratio for better identification of interannual and decadal variability in the data.

[17] The overall linear trends of all series in this paper were calculated over the 1961–2004 period by means of least squares linear fitting, and their significance estimated by the Mann-Kendall nonparametric test at the 5% level of confidence. Also, all time series shown in this paper are plotted together with their 11-a window 3- $\sigma$  Gaussian low-pass filter for a better visualization of long-term and decadal variability.

### 2.3. Classification of Atmospheric Circulation Patterns in the Euro-Atlantic Sector

[18] The analysis of the circulation patterns was performed on seasonal mean sea level pressure (SLP) provided by the National Center for Atmospheric Research (NCAR) on a regular  $5^\circ \times 5^\circ$  grid [Trenberth and Paolino, 1980] (data available at <http://dss.ucar.edu/datasets/ds010.1>). We selected a window over the Euro-Atlantic sector ( $50^\circ\text{W}$ – $40^\circ\text{E}$ ;  $20^\circ\text{N}$ – $70^\circ\text{N}$ ) during the same 1961–2004 period that covers the SunDu and TCC series. We discarded the annual basis analysis since there are important differences in the variability and modes of circulation patterns along the year [Barnston and Livezey, 1987].

[19] Unrotated PCA in S-mode [Preisendorfer, 1988] was applied to the seasonal anomalies of SLP, using the correlation matrix in order to ensure the inclusion of the lower variance in the lower latitudes of our domain [Barnston and

Livezey, 1987]. Under the S-mode approach, clusters of grid points with similar time behaviors are obtained by the principal component (PC) loadings, and the structure of the time behavior is categorized by the PC scores. Thus, the obtained results can be interpreted as teleconnections or atmospheric circulation patterns that capture the leading modes of SLP variability [Huth, 2006]. We repeated the analyses by using the covariance matrix and similar results were obtained (not shown). The number of components to be retained was determined from the eigenvalue versus PC number plots (Scree Test), assuming that the convenient choice is indicated by the end of a section with a small slope that is followed by a pronounced drop [O’Lenic and Livezey, 1988]. Also, a minimum of 70% of the total explained variance in the retained components [Briffa *et al.*, 1994] was required.

[20] Since unrotated S-mode PCA can produce artifacts in the results, we rotated the retained components. The rotation produces real physical patterns with more statistically robust solutions [Huth, 2006], with a redistribution in the final explained variance between the rotated components that enables to a clearer separation of components and concentrates the loadings for each component into the most influential variables. We used the Varimax rotation which is the most widely applied and recommended option for circulation pattern classification [Barnston and Livezey, 1987; Huth, 2006]. Subsequently, we estimated, by regression of the loadings for each rotated EOF, the PC time series (scores) that characterize the EOF time behavior during the analyzed period.

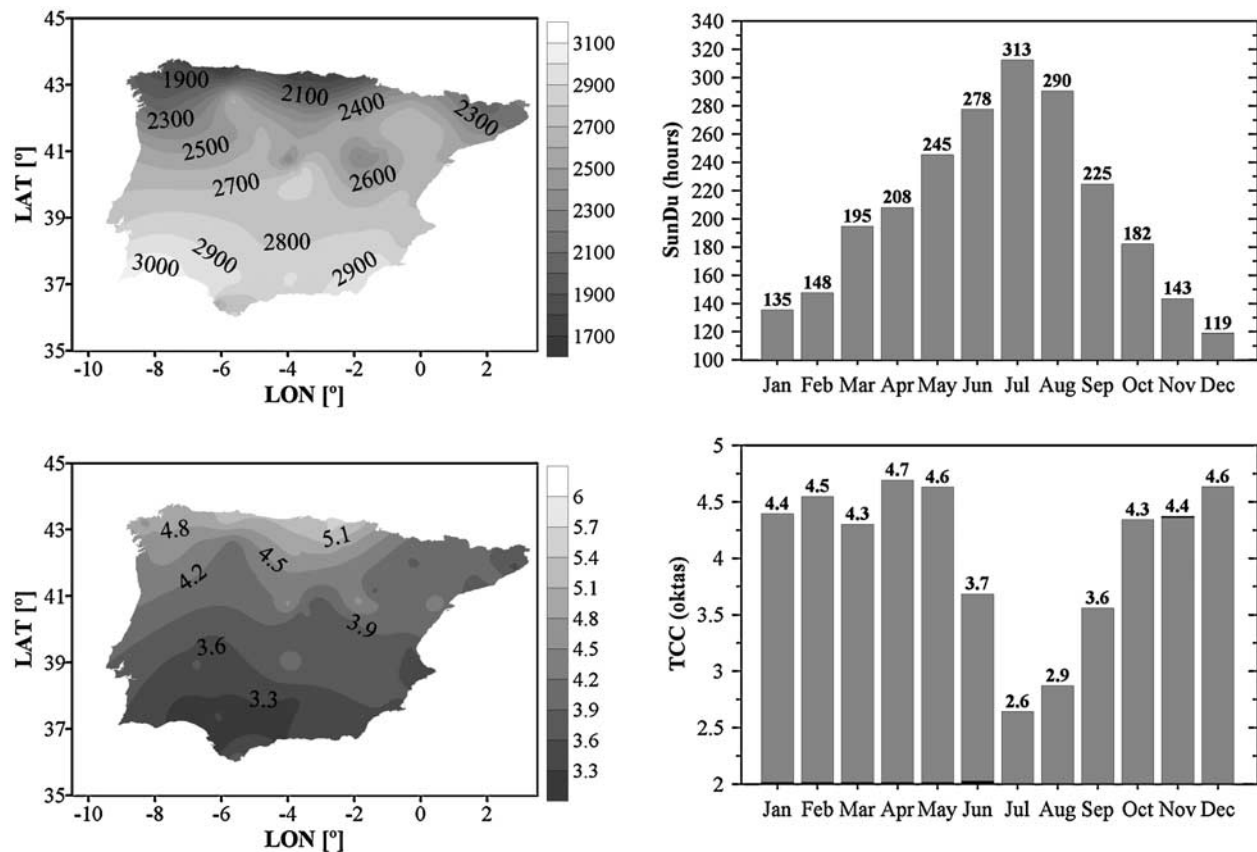


**Figure 2.** (left) Mean annual (top) SunDu and (bottom) TCC and (right) the corresponding mean monthly course over the IP during the 1971–2000 period.

[21] We have also computed one-point correlation maps between the SunDu (or TCC) series and the gridded SLP time series for the 1961–2004 period. The aim of these analyses is to give a more direct assessment of the role of SLP variations in SunDu and TCC variability over the IP, and also to verify the results based on PCA.

### 3. Sunshine Duration, Total Cloud Cover, and Dimming/Brightening Trends

#### 3.1. Spatial and Temporal Comparison of Sunshine Duration and Cloudiness

[22] Figure 2 shows the interpolated maps of the mean annual series of SunDu and TCC (left), with their mean monthly course over the whole IP (right) for the 1971–2000 period. The annual SunDu and TCC maps show a similar but opposite pattern and clear latitudinal dependence, with SunDu (TCC) less (more) than 2000 h per year (4.5 oktas) in the northern area and more (less) than 2800 h per year (3.5 oktas) in the southern sectors of the IP. Besides this zonal mean pattern there is a slight influence of the Atlantic Ocean since SunDu (TCC) isolines indicate, for a given latitude, lower (higher) values in the west compared to the east. The mean seasonal cycles of SunDu and TCC are out-of-phase. SunDu reaches maximum values during summer (more than 275 h per month during June, July, and August), and minimum values in winter (less than 150 h per month during November, December, January, and February). This is obviously related with the astronomical course of the Sun

in these latitudes, but it might be also influenced by varying cloudiness. Indeed, TCC shows a minimum in summer, with less than 3 oktas in July and August, but there is not a clear maximum since several winter and spring months (from October to May) reach more than 4 oktas. It is important to highlight that SunDu annual mean is more influenced by the summer than by the other seasons while the opposite is true for TCC.

[23] Figure 3 shows the relationship between annual and seasonal SunDu and TCC anomalies for all IP cells during the 1961–2004 period, and the linear regressions of these points are also shown to represent the mean behavior of SunDu in relation with TCC. For the annual data (Figure 3a), the correlation coefficient between the SunDu and TCC is  $-0.54$  ( $\alpha \leq 0.01$ ). On the other hand, during winter (Figure 3b) the correlation coefficient increases to  $-0.88$  ( $\alpha \leq 0.01$ ), so an excellent fit between the values exists. In addition, in winter most data are close to the diagonal line. Meanwhile, for summer (Figure 3d) the correlation coefficient decreases to  $-0.62$  (although it is also significant at the  $\alpha \leq 0.01$  level). As in the annual scatterplot, during summer the points do not fall symmetrically around the diagonal line. For spring ( $r = -0.79$ ,  $\alpha \leq 0.01$  level) and autumn ( $r = -0.80$ ,  $\alpha \leq 0.01$  level) the behavior is similar, but in an intermediate state between winter and summer. The SunDu anomalies in excess of the expected values, in cases of high TCC anomalies, might be related to the well-known tendency of ground-based

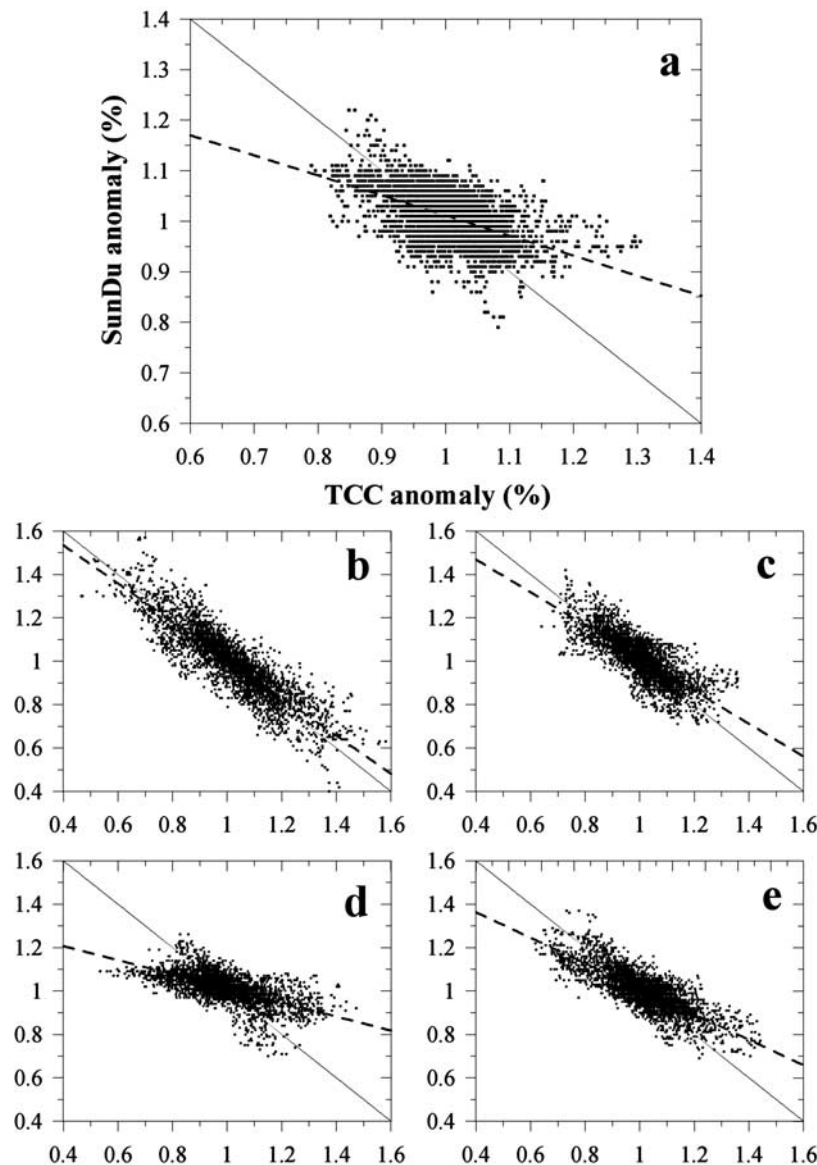


**Figure 3.** Relationship between SunDu and TCC, where each point is the mean for 1 year's data at one grid point during the 1961–2004 period ((a) annual, (b) winter, (c) spring, (d) summer, and (e) autumn). The values are expressed as relative deviations from the 1971–2000 mean and the linear regression is indicated in each plot.

observers to overestimate the TCC because of their inability to detect fractional cloudiness when clouds have significant vertical extent, a factor that is more important during summer over the IP when most clouds are of convective origin instead of frontal origin [Angell *et al.*, 1984]. In contrast, when SunDu anomalies are underestimated, for lower TCC anomalies, the cause may be related to atmospheric aerosols which reflect and absorb solar radiation and reduce the amount of direct solar radiation reaching the Earth's surface [Stanhill, 2003]. As shown in Figure 3, this phenomenon is especially important during the summer, the period of the year which shows the greatest aerosol concentrations over the IP [Papadimas *et al.*, 2008].

[24] Figure 4 shows the local correlation coefficients between SunDu and TCC over the IP based on annual and seasonal data, using interpolated values obtained at each grid

point. All correlation coefficients exceed the 95% significance level. For the annual map (Figure 4a), the greater values in the northern sectors of the IP are in contrast with the lower correlations obtained in the southern areas. Note that the annual values are not representative for the whole year, since for winter, spring, and autumn there are in general greater values ( $r > 0.8$ ) for the whole IP. This indicates that a major part of the interannual variation in SunDu is probably a result of cloudiness variations. On the other hand, in summer (Figure 5d) there is also high correlation in the northwestern sectors, but the values decrease clearly in the southern area. Consequently, SunDu variance explained by TCC is lower, which may be related to the different nature (more convective and fractional) of summer cloudiness, or to the effect of higher aerosol concentrations (dust, smoke, and/or haze) [Papadimas *et al.*, 2008].

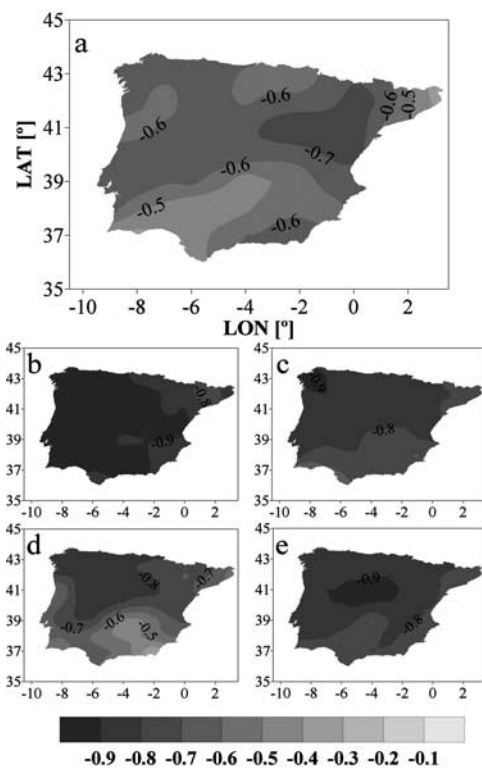


**Figure 4.** Pearson's correlation coefficient between SunDu and TCC series during the 1961–2004 period ((a) annual, (b) winter, (c) spring, (d) summer, and (e) autumn). Absolute values greater than 0.40 are statistically significant at the 1% level.

[25] Figure 5 shows the mean annual and seasonal time evolution series for SunDu and TCC (with reversed axis) for the whole IP. These mean series are significantly correlated, as it was obtained from the scatterplots considering all grid points (Figure 3). Thus, for the annual series (Figure 5a) there is a correlation of  $-0.60$  ( $\alpha \leq 0.01$ ); note however that there is a clear disagreement between both series from the 1960s to mid-1980s. Thus, SunDu shows a clear decrease, or dimming, during this subperiod while TCC shows a stabilization or slight decrease that does not match with the behavior of SunDu. After the mid-1980s there is a good agreement between both variables since SunDu (TCC) increases (decreases) until 2000, and then show a new slight decrease (increase) during the more recent years. Also, it is very remarkable that the SunDu absolute minimum reached in 1982–1984 does not correspond with high TCC anomalies (values are below the 1971–2000 mean). Regarding long-term trends over the 1961–2004 period, SunDu series shows a slightly negative, nonsignificant value, while for TCC there is a significant decrease of  $-1.4\%$  per decade.

[26] In winter (Figure 5b) the SunDu and TCC time series match almost perfectly ( $r = -0.95$ ), and, in contrast to the annual series, there is no disagreement between SunDu and TCC series during the first half of the analyzed period. Both linear trends over the 1961–2004 period are not significant. During spring, there is a high correlation between SunDu and TCC series ( $r = -0.87$ ), but also a clear discrepancy during the 1960–1980 period: as in the annual series, there

is a clear dimming in SunDu while TCC remains relatively constant. In this season we also detect a clear minimum in the SunDu anomalies (1982–1984), which is not clearly marked in the TCC series. As a consequence of these differences, the linear trend for the whole analyzed period is not significant for the SunDu series but there is a significant TCC decrease of  $-2.2\%$  per decade. This disagreement is enhanced during summer, with a slight decrease in the correlation ( $r = -0.73$ ) and again a decrease in SunDu during the 1960–1980s period that is not associated with an increase in TCC. Both linear trends show negative nonsignificant values. Finally, in autumn both series match quite well, similarly to the winter series ( $r = -0.88$ ). The subregional analysis show similar results to the mean IP series following the spatial and temporal signals detected in Figures 4 and 5.

### 3.2. Residual Anomalies Between SunDu and TCC

[27] Summarizing the previous section, TCC variability accounts for much of the SunDu variability over the IP on interannual and decadal time scales. However, there is a fraction of SunDu variability that cannot be explained by TCC variability (especially during spring and summer), and other factors, such as changes in aerosol optical thickness (AOT), may be important to understand the variations of solar radiation reaching the surface. In fact, the variability in AOT is relatively small in comparison to mean cloud optical thickness values and variability; consequently, direct radiative forcing by aerosols is much lower in overcast than in clear sky conditions because the incoming solar radiation is scattered or absorbed by clouds instead of by aerosols [Norris and Wild, 2007]. In order to remove the cloud effect and detect a dimming or brightening signal linked to other factors, and similarly to other authors [e.g., Wild et al., 2005; Norris and Wild, 2007] we obtained the residual series by simply subtracting the expected SunDu (according the observed TCC anomalies) from the measured SunDu. Specifically, for the annual and seasonal basis, we used the linear regressions showed in Figure 3 and then we subtracted the expected SunDu anomalies from the observed SunDu anomalies. In order to simplify the interpretation of the results, we avoided possible subregional differences and the residual series was obtained only for the whole IP. The residual annual and seasonal time series are all significantly ( $\alpha \leq 0.01$ ) correlated, with correlation coefficients greater than 0.70 except between spring and winter ( $r = 0.54$ ) and spring and autumn ( $r = 0.64$ ).

[28] The annual residual series for the whole IP shows a clear decrease from the 1960s to the beginning of the 1980s with a subsequent recovery to the 2000s punctuated by two distinct minima in 1982–1985 and in 1992–1993 (Figure 6a). Thus, after removing the TCC effect, there is a clear decrease (increase) in SunDu anomalies during the first (last) two decades that cannot be explained by TCC. The two pronounced minima are remarkable, and likely related to the El Chichón (April 1982) and Pinatubo (June 1991) large volcanic eruptions. In fact, it is well known that the global effects of a large volcanic eruption are caused by droplets of sulfuric acid that efficiently scatter shortwave radiation, inducing a decrease (increase) of the amount of direct (diffuse) solar radiation reaching the surface and leading to cooling [Robock, 2000]. The seasonal residual time series are similar in shape to the annual residual record (Figures 6b–6e). The

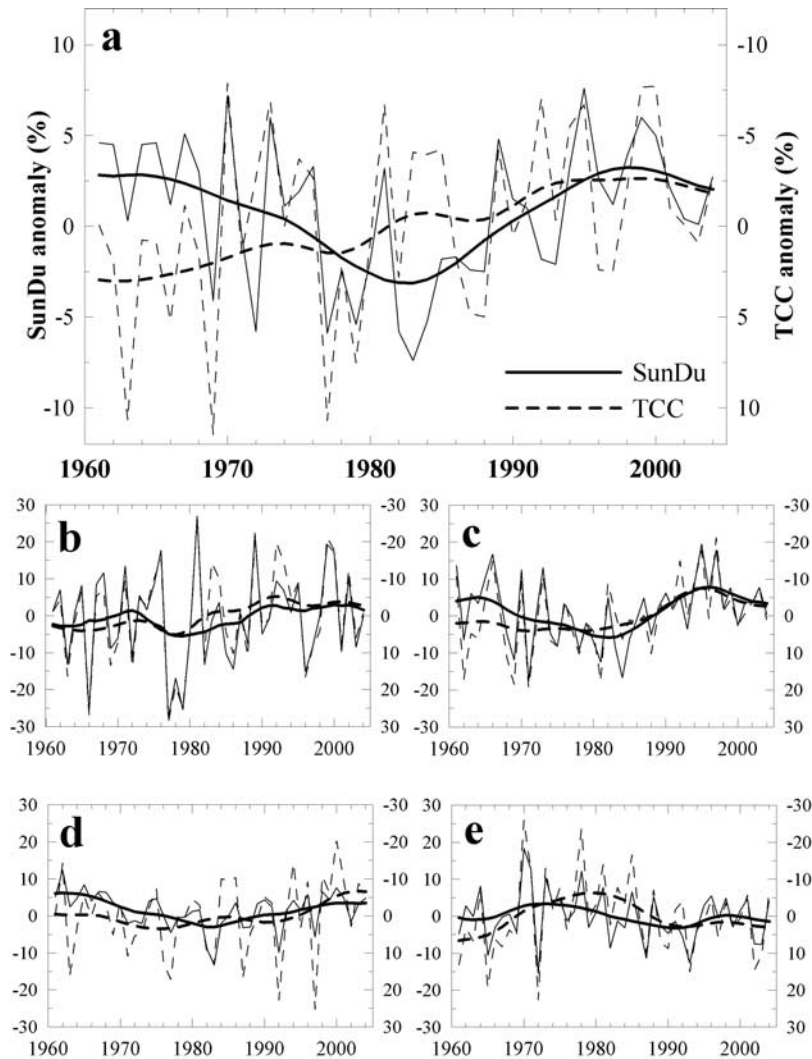


**Figure 5.** Annual and seasonal time evolution of both SunDu (solid lines) and TCC (dashed lines) series (thin lines) for the whole IP during the 1961–2004 period, plotted together with the 11-a window 3- $\sigma$  Gaussian low-pass filter (thick lines; (a) annual, (b) winter, (c) spring, (d) summer, and (e) autumn). The series are expressed as relative deviations (%) from the 1971–2000 mean. Note that the scale for TCC series has a reversed axis.

low values reached during 1982–1984 are also noteworthy in all seasons although they are clearer during spring and summer; the other minimum reached during 1992–1993 is clear in all seasons but summer. Linear trends over the period as a whole are negative and significant only in the winter and summer series (similar results hold if the years 1982–1984 and 1992 are eliminated from the analyses).

[29] A limitation in the previous residual anomalies series is the difficulty in expressing the changes in suitable units. Another limitation is related to the fact that the residual series combine variations in clear sky solar radiation flux with variations in cloud optical thickness that are unrelated to cloud cover [Norris and Wild, 2007]. In order to confirm the possibility of a direct aerosol effect in the residual series we calculated the SunDu mean for clear sky conditions. Since this analysis is based on daily data, we only selected the completely homogeneous series in both SunDu and TCC variables and containing at least 30 years of data in daily

resolution during the 1961–2004 period. These restrictions resulted in a selection of only 11 stations, which fortunately are well distributed across the IP. In these series, a day was defined as clear if the mean TCC from the 3 daily observations is less than 1.5 oktas, following the criterion established by AEMET. The annual and seasonal mean IP series were obtained by averaging the 11 SunDu anomalies (obtained as differences to the corresponding 1971–2000 mean) series expressed in hours per day, for the clear sky days selected in each station. The mean IP annual SunDu for clear sky conditions (Figure 7a) shows a decrease from the 1960s to the beginning of the 1980s, with a minimum in 1983. Afterward a positive trend appears up to the end of the analyzed period, only interrupted by another relative minimum in 1992. The seasonal time series show positive significant correlations ( $r \geq 0.50$ ,  $\alpha \leq 0.01$ ) and a temporal behavior that resembles the annual series, although for spring and summer there is a more obvious minimum at the

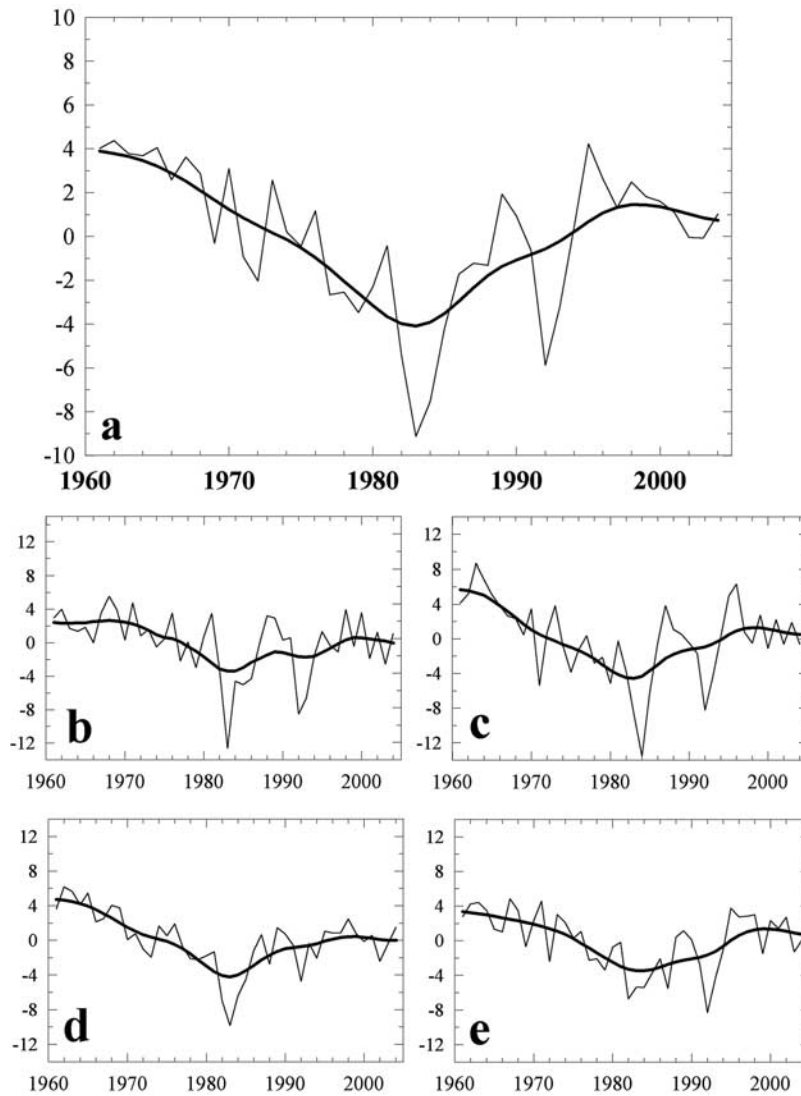


**Figure 6.** IP residual anomalies after removing the TCC effect in the SunDu series (thin line), plotted together with the 11-a window  $3\text{-}\sigma$  Gaussian low-pass filter (thick line), during the 1961–2004 period ((a) annual, (b) winter, (c) spring, (d) summer, and (e) autumn). The series are expressed as relative deviations (%) from the 1971–2000 mean.

beginning of the 1980s and a more constant decrease and increase during the first and last two decades, respectively. Finally, neither the annual nor the seasonal series show any significant trend over the period of record. These mean IP SunDu series under cloud free days were correlated with the residual series, and consistently we found highly significant correlations ( $r \geq 0.65$ ,  $\alpha \leq 0.01$ ) both at annual and seasonal basis.

#### 4. SunDu and TCC Relationships With Atmospheric Circulation Patterns

[30] To assess the linkages between atmospheric circulation variations and TCC/SunDu changes, we have computed one-point correlation maps between gridded SLP anomalies over the Euro-Atlantic sector and the IP TCC and SunDu series for each season separately (Figure 8). As expected, the patterns and amplitudes of the SLP correlation maps are

nearly equal and opposite for TCC and SunDu. Locally over the IP, above (below) normal SLP is associated with below (above) normal TCC and above (below) normal SunDu in all seasons, consistent with synoptic experience. The local SLP anomalies are part of a more extensive pattern in all seasons except summer. For example in winter, the SLP correlation pattern consists of a zonally elongated north-south dipole extending over the entire Euro-Atlantic domain with a nodal line near  $55^\circ\text{N}$ . This pattern bears some resemblance to the NAO but it is shifted northward by  $\sim 5\text{--}10^\circ$  of latitude. A similar although spatially more confined SLP dipole pattern occurs in spring and to a lesser extent in autumn. The amplitudes of the SLP correlation coefficients are generally greatest in winter (maximum values  $\sim 0.8$ ) and smallest in summer (maximum values  $\sim 0.5$ ), well in excess of the 0.05 significance value of  $\sim 0.3$ . In summary, interannual and decadal variations in TCC and SunDu over the IP are associated with local changes in SLP

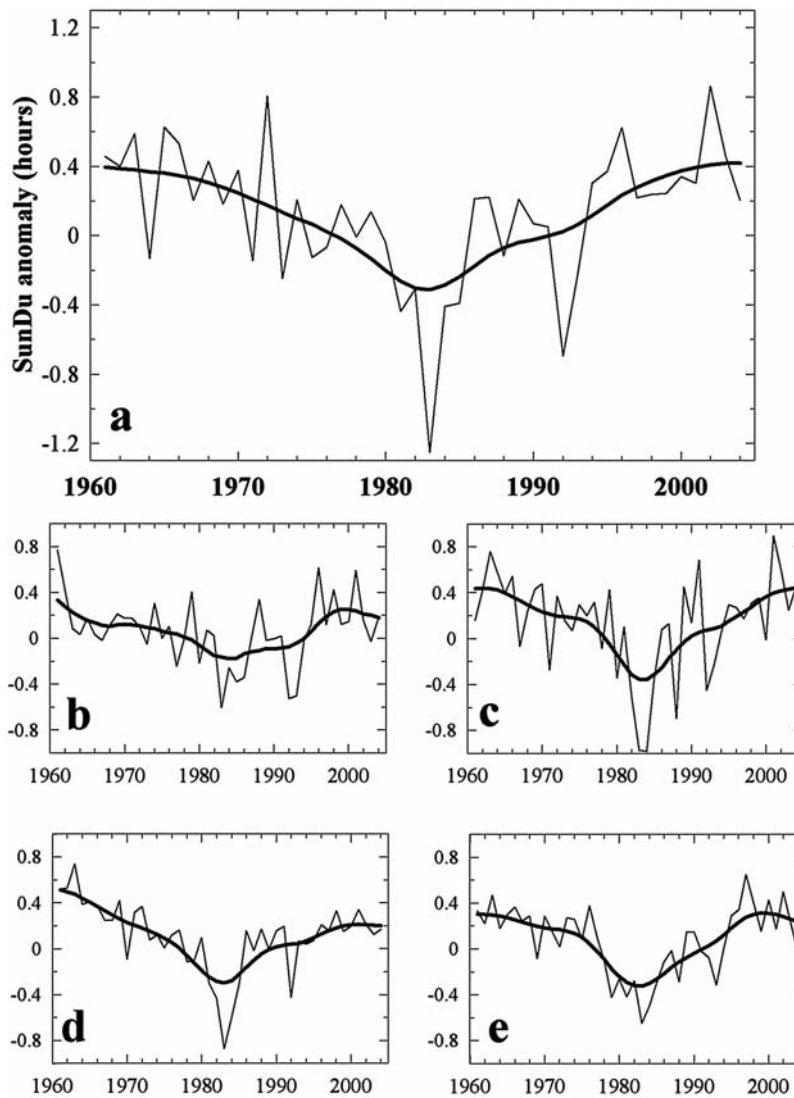


**Figure 7.** Daily mean SunDu (hours) series over the IP for cloud-free sky conditions (thin line), plotted together with the 11-a window 3- $\sigma$  Gaussian low-pass filter (thick line; (a) annual, (b) winter, (c) spring, (d) summer, and (e) autumn). The series are expressed as daily SunDu anomalies (hours) from the 1971–2000 mean.

in all seasons, and with anomalous large-scale atmospheric circulation patterns in all seasons except summer. The seasonal one-point SLP correlation maps based on the residual SunDu record (not shown) are considerably weaker than those based on the original TCC and SunDu records.

[31] Next, we examined the relationships between preferred patterns of atmospheric circulation variability and the TCC/SunDu records over the IP. To determine the dominant patterns of atmospheric circulation variability over the Euro-Atlantic sector, we applied a separate rotated PCA to the gridded SLP anomalies in each season. The number of EOFs retained in the rotated PCA (and their total variance explained) are four (82%) for winter, six (80%) for spring, eight (81%) for summer, and eight (85%) for autumn. We then correlated the PC time series associated with each rotated EOF with the SunDu, TCC, residual SunDu, and clear sky SunDu time series for the whole IP and the four IP subregions (Table 1). Only those EOFs that are significantly correlated with SunDu or TCC are discussed.

[32] In winter, PC1 and PC4 are significantly correlated ( $\alpha \leq 0.01$ ) with the SunDu (positive correlation) and TCC (negative correlation) series over the IP and over most of the IP subregions. In its positive phase, EOF1 (Figure 9a) is defined by high- and low-pressure systems over the Mediterranean basin and northern Europe, respectively. This dominant mode of winter SLP variability has been detected previously over a similar domain [Slonosky *et al.*, 2000; Rimbu *et al.*, 2006], an aspect that contrasts with other analyses applied over greater domains where other modes (specifically, the North Atlantic Oscillation, NAO) are detected as the leading mode of variability [Hurrell *et al.*, 2003]. In fact, in our analyses, EOF2 (not shown) represents the well-known spatial structure of the NAO, although with a westward displacement, and its PC series is not significantly correlated with either SunDu or TCC. However, both rotated PC1 ( $r = 0.68$ ) and PC2 ( $r = 0.56$ ) are highly correlated with the NAO index [Jones *et al.*, 1997] indicating that both circulation patterns are regional manifestations

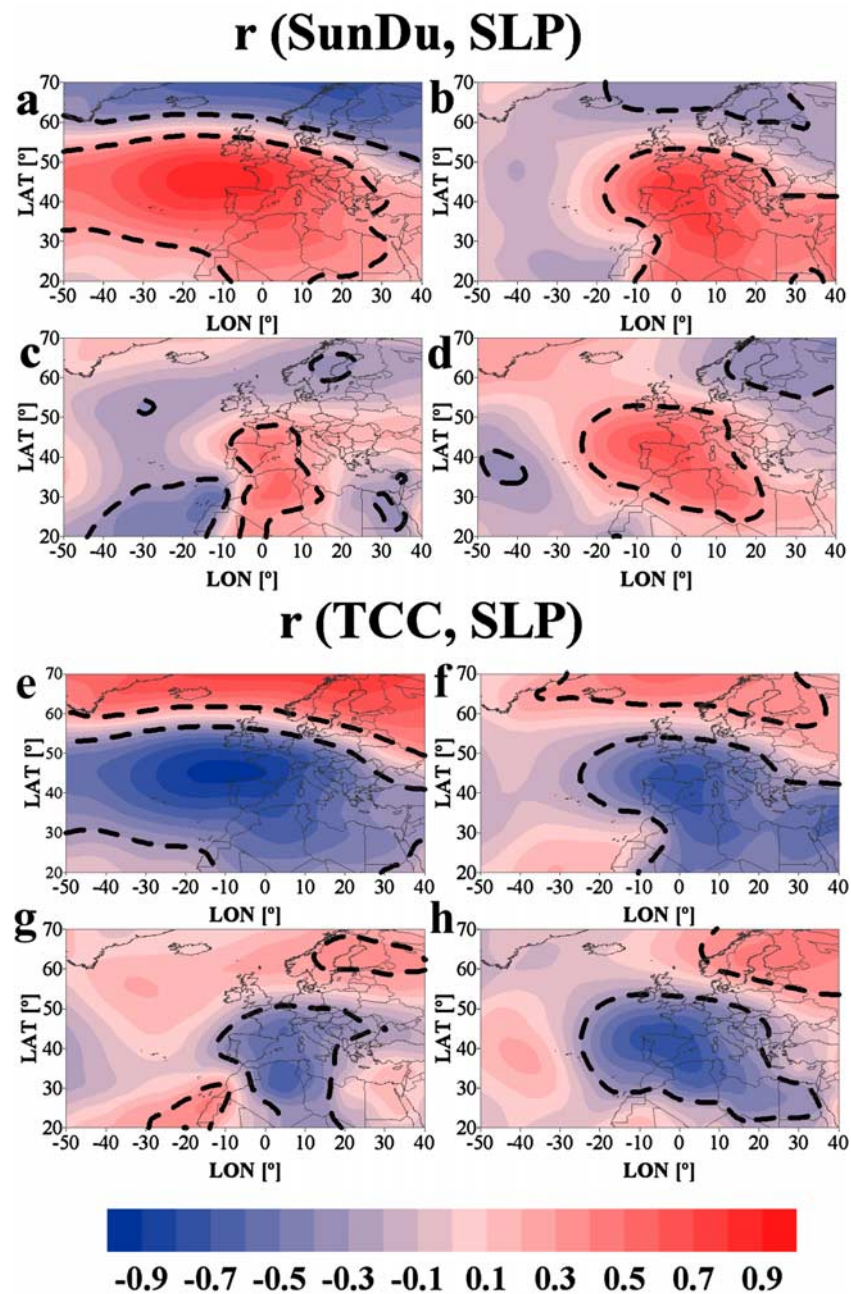


**Figure 8.** Spatial distribution of correlations between SLP and the mean IP (top) SunDu and (bottom) TCC series ((a and e) winter, (b and f) spring, (c and g) summer, and (d and h) autumn). The dashed contours indicate approximate 95% significant levels ( $|r| \geq 0.30$ ,  $\alpha \leq 0.05$ ).

of the NAO. These results help to reconcile the results based on one-point SLP correlation maps (Figure 8a) and are consistent with previous findings [Pozo-Vázquez *et al.*, 2004; Sanchez-Lorenzo *et al.*, 2008a], that established a highly significant positive correlation between the NAO and the sunshine duration in southern Europe. PC4 (Figure 9c) also shows significant correlations with SunDu and TCC, except for the N subregion. During the positive phase of this circulation pattern there is anomalous high pressure over the Atlantic Ocean centered north of the Azores islands. This circulation pattern, which does not exhibit a dipole configuration, is not significantly correlated with the NAO index.

Finally, PC3 (Figure 9b) has significant ( $\alpha \leq 0.05$ ) positive (negative) correlations with the SunDu (TCC) series only for subregions N and W. This pattern shows a single-cell structure centered over Central Europe which, during its positive phase, is associated with anomalous easterly flow over the IP. Under these conditions, while the eastern and southern regions of the IP receive humid air, the remaining parts of the IP (west and north) are notably dry [Lopez-Bustins *et al.*, 2008]. In general, similar winter trends and atmospheric circulation influence in TCC can be observed for the IP in the context of the whole Mediterranean basin and using the data NCEP/NCAR reanalysis data set [Lolis, 2009].

**Table 1.** Correlation Coefficients Between the PC Time Series of Rotated SLP EOFs Over the Euro-Atlantic Sector and the Time Series of SunDu, TCC, SunDu Residual and SunDu Clear Sky Over the IP and the Four IP Subregions<sup>a</sup>

SLP EOF	SLP %Variance	SunDu					TCC					IP SunDu Residual	IP SunDu Clear Sky
		IP	E	N	W	S	IP	E	N	W	S		
<i>Winter</i>													
1	28.5	<b>.52</b>	<b>.50</b>	<b>.52</b>	<i>.38</i>	<b>.52</b>	<i>-.57</i>	<i>-.57</i>	<i>-.56</i>	<i>-.45</i>	<i>-.58</i>	–	–
3	15.5	+	–	<b>.51</b>	<i>.38</i>	–	–	–	<i>-.62</i>	<i>-.41</i>	–	–	–
4	14.9	<b>.63</b>	<b>.62</b>	+	<b>.65</b>	<b>.59</b>	<i>-.65</i>	<i>-.64</i>	–	<i>-.64</i>	<i>-.66</i>	+	–
<i>Spring</i>													
1	42.3	<b>.69</b>	<b>.68</b>	<b>.72</b>	<b>.54</b>	<b>.62</b>	<i>-.64</i>	<i>-.64</i>	<i>-.65</i>	<i>-.51</i>	<i>-.61</i>	+	+
4	16.8	–	–	–	–	–	–	–	+	–	–	<i>-.54</i>	<i>-.44</i>
<i>Summer</i>													
2	26.6	<i>.32</i>	<i>.34</i>	+	<i>.36</i>	+	<i>-.45</i>	<i>-.42</i>	<i>-.48</i>	<i>-.51</i>	–	+	–
5	20.7	<i>-.53</i>	<i>-.45</i>	<i>-.46</i>	<i>-.46</i>	<i>-.44</i>	+	+	<i>.30</i>	<i>.31</i>	+	<i>-.54</i>	<i>-.43</i>
<i>Autumn</i>													
5	20.0	<i>.33</i>	+	<i>.37</i>	+	+	<i>-.43</i>	<i>-.38</i>	<i>-.41</i>	<i>-.37</i>	<i>-.42</i>	–	–
6	19.8	<i>-.30</i>	<i>-.36</i>	–	–	–	+	+	+	+	+	<i>-.42</i>	<i>-.39</i>
7	17.2	<b>.51</b>	<b>.46</b>	–	<b>.50</b>	<b>.74</b>	<i>-.54</i>	<i>-.47</i>	–	<i>-.51</i>	<i>-.65</i>	+	–

<sup>a</sup>Only those EOFs that are significantly correlated with the SunDu and/or TCC records are shown. Correlation coefficients significant at  $\alpha \geq 0.01$  ( $\alpha \geq 0.05$ ) are shown in bold (italics); values with lower levels of significance are indicated by sign (+ or –) only.

Neither the residual nor the clear sky SunDu series exhibit significant correlations with any of the winter SLP EOFs. Regarding long-term trends, although EOF1 shows a slightly increase, none of the three PC time series (Figure 9) has significant trends.

[33] In spring, the leading EOF (Figure 10a) represents a similar spatial structure as the leading EOF in winter, and consequently can also be considered as a regional manifestation of the NAO. The PC series of this pattern shows positive (negative) significant correlations ( $\alpha \leq 0.01$ ) with SunDu (TCC) series for the whole IP and all subregions. Moreover, a clear increase of this pattern is detected from the 1980s, resulting in a positive significant trend over the analyzed period. This significant positive increase agrees with the significant decrease in TCC detected over the whole IP. Similar to winter, EOF2 (not shown) represents the typical NAO pattern configuration, with the Icelandic low and the Azores high centers of action. But, as in winter, this pattern does not have significant correlations with SunDu and TCC series; the same is true for the remaining circulation patterns. Another relevant result during spring is the significant negative correlations ( $\alpha \leq 0.01$ ) between PC4 (Figure 10b) and the residual ( $r = -0.52$ ) and clear sky SunDu ( $r = -0.44$ ) series. The positive phase of this pattern is characterized by a single-cell high-pressure system over the central North Atlantic Ocean (somewhat similar to the spatial configuration of winter EOF4, Figure 9c), which may be regarded as a blocking situation. However, the physical connection between this pattern and the residual or clear sky series is not understood. In agreement with the residual and clear sky SunDu series, PC4 shows a general upward trend from the 1960s to 1980s with a subsequent decrease to the present.

[34] During summer, the relationships between SunDu or TCC and the dominant modes of atmospheric circulation variability are generally weaker than in winter and spring. This is understandable given that clouds have a more convective as opposed to dynamical origin in the warm season. In summer, PC2 (Figure 11a) is most strongly correlated with TCC while PC5 (Figure 11b) is most strongly correlated with

SunDu. In its positive phase EOF2 exhibits an anomalous anticyclone centered over the Mediterranean basin which promotes sunnier and less cloudy conditions. The positive phase of EOF5 exhibits an anomalous anticyclone over the Atlantic Ocean northwest of Africa, with an anticyclonic ridge that extends northeastward up to the IP. This pattern is significantly negatively correlated ( $\alpha \leq 0.01$ ) with the summer SunDu residual ( $r = -0.54$ ) and clear sky SunDu ( $r = -0.43$ ) records. As in spring with EOF4 (Figure 10b), there is not a clear physical explanation for the connection between this anomalous SLP pattern and the SunDu records. PC5 shows an increase from the 1960s to 1980s, with a tendency toward more negative phases during the last two decades.

[35] In autumn, the strongest linkages between SunDu or TCC and preferred atmospheric circulation patterns occurs for PC7 (Figure 12c). The positive phase of this pattern is characterized by a high-pressure system over the southwestern IP, which generates stable and fair weather conditions, consistent with the sign of the correlations in Table 1. Contrarily, during the negative phase there is a low-pressure system that generates an important cyclogenesis with a southern flow over the IP that invigorates convective cloudiness and rainfall. In fact, EOF7 resembles the Western Mediterranean Oscillation (WeMO) identified by *Martin-Vide and Lopez-Bustins* [2006] and is significantly correlated ( $r = 0.63$ ,  $\alpha \leq 0.01$ ) with the WeMO index (<http://www.ub.es/gc/English/wemo.htm>). Also PC5 (Figure 12a) exhibits significant ( $\alpha \leq 0.05$ ) positive (negative) correlations with the IP SunDu (TCC) series. The positive phase of this pattern exhibits an anomalous anticyclonic system over the central Mediterranean basin and the north part of Africa. The well-known impact of this type of circulation pattern [*Escudero et al.*, 2005] is an increase in African dust intrusions (increasing AOT) over the IP. This may reduce the direct solar radiation down to values lower than the threshold required to mark the sunshine duration recorder, thus explaining the nonsignificant correlations with many of the regional SunDu series. Finally, the autumn PC6 (Figure 12b), whose associated EOF resembles the spatial configuration of

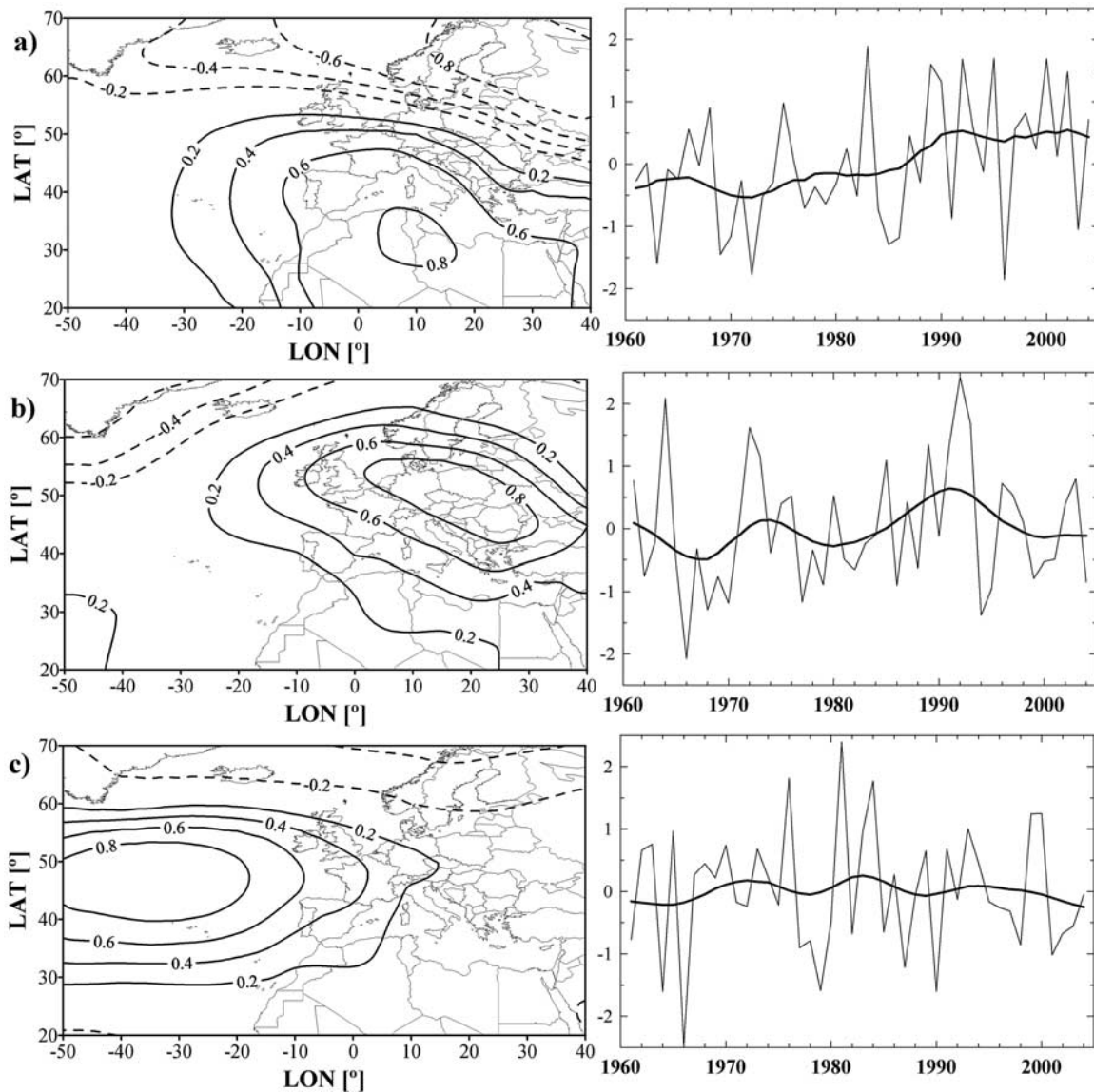


**Figure 9.** (left) Three EOFs of the winter SLP anomalies over the Euro-Atlantic sector displayed as PC loading. Negative loadings are dashed, the contour increment is 0.2, and the zero contour has been excluded. (right) PC time series of each EOF (thin line), plotted together with the 11-a window 3- $\sigma$  Gaussian low-pass filter (thick line; (top) EOF1, (middle) EOF3, and (bottom) EOF4).

EOF5 in summer (Figure 11b), exhibits significant correlations with the residual SunDu ( $r = -0.42$ ,  $\alpha < 0.01$ ) and clear sky SunDu ( $r = -0.39$ ,  $\alpha \leq 0.01$ ) series. These results confirm the relationship between this mode of atmospheric circulation and the dimming/brightening phenomena over the IP. The PC series of this pattern, which does not have a significant trend over the analyzed period, shows an increase in its positive phase during the 1970s and early 1980s, with a decrease until the end of the 20th century.

## 5. Conclusions

[36] We have presented in this paper a spatial and temporal comparison between sunshine duration and total cloud cover over the Iberian Peninsula, on the basis of homogenized and gridded data sets obtained from about 70 instrumental series

covering the period 1961–2004. We took special care to reduce the inhomogeneities in the original data, since otherwise the partial subjectivity of conventional cloudiness observations could have introduced important biases in the final results, especially in long-term estimations.

[37] As in previous studies in different areas of the world [e.g., Angell, 1990; Jones and Henderson-Sellers, 1992], we detected a negative and highly significant correlation between both variables, although lower correlations were found for the spring and summer series, compared with winter or autumn data. In general, the correlations are lower in the southern sectors of the IP than in the north. On the basis of the long-term comparison, it is clear that the most important discrepancy between SunDu and TCC is detected from the 1960s until the early 1980s, particularly during spring and summer; specifically, SunDu shows a clear decrease that is

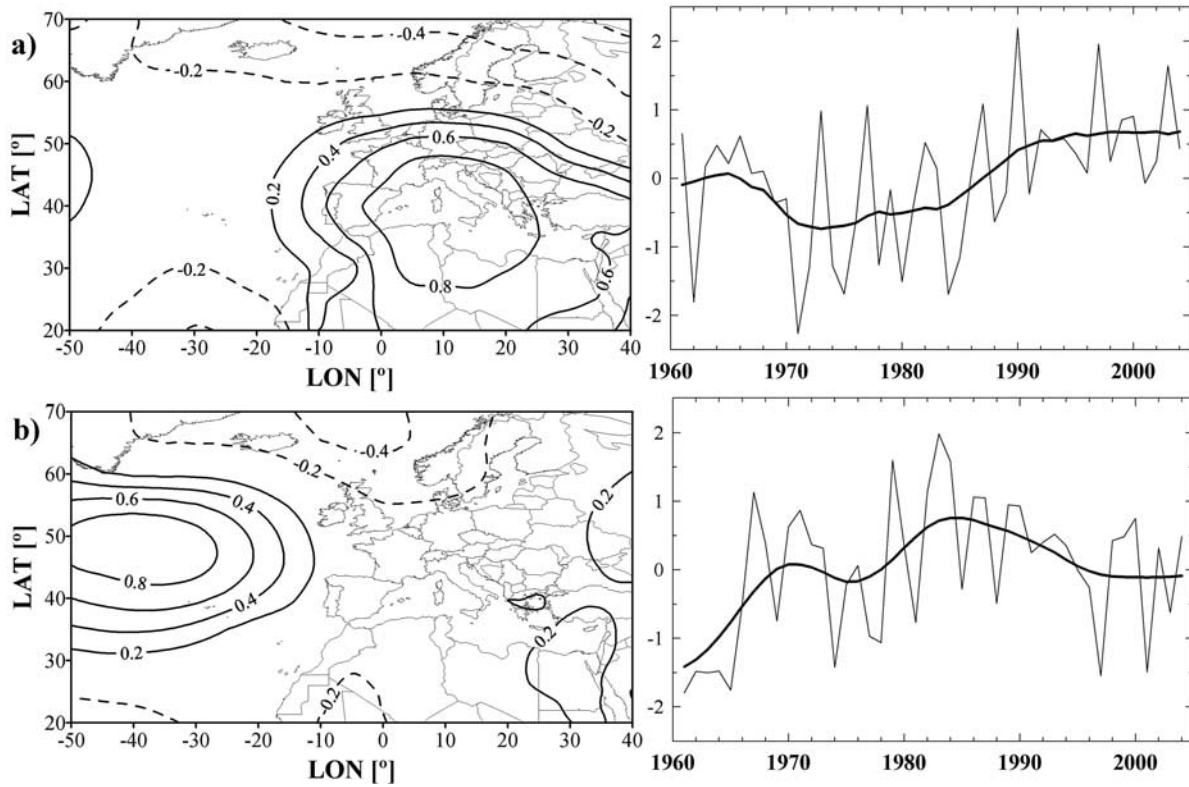


Figure 10. As in Figure 9 but in spring, and for two EOFs ((a) EOF1 and (b) EOF4).

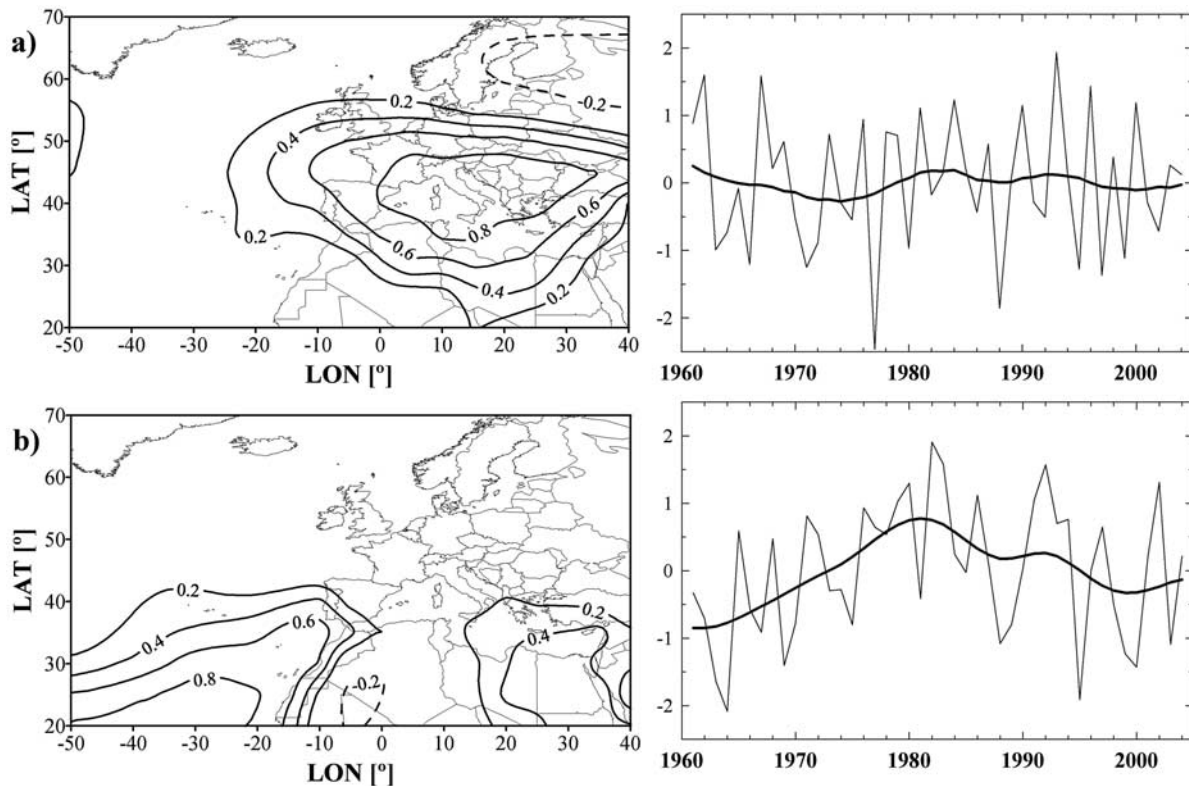
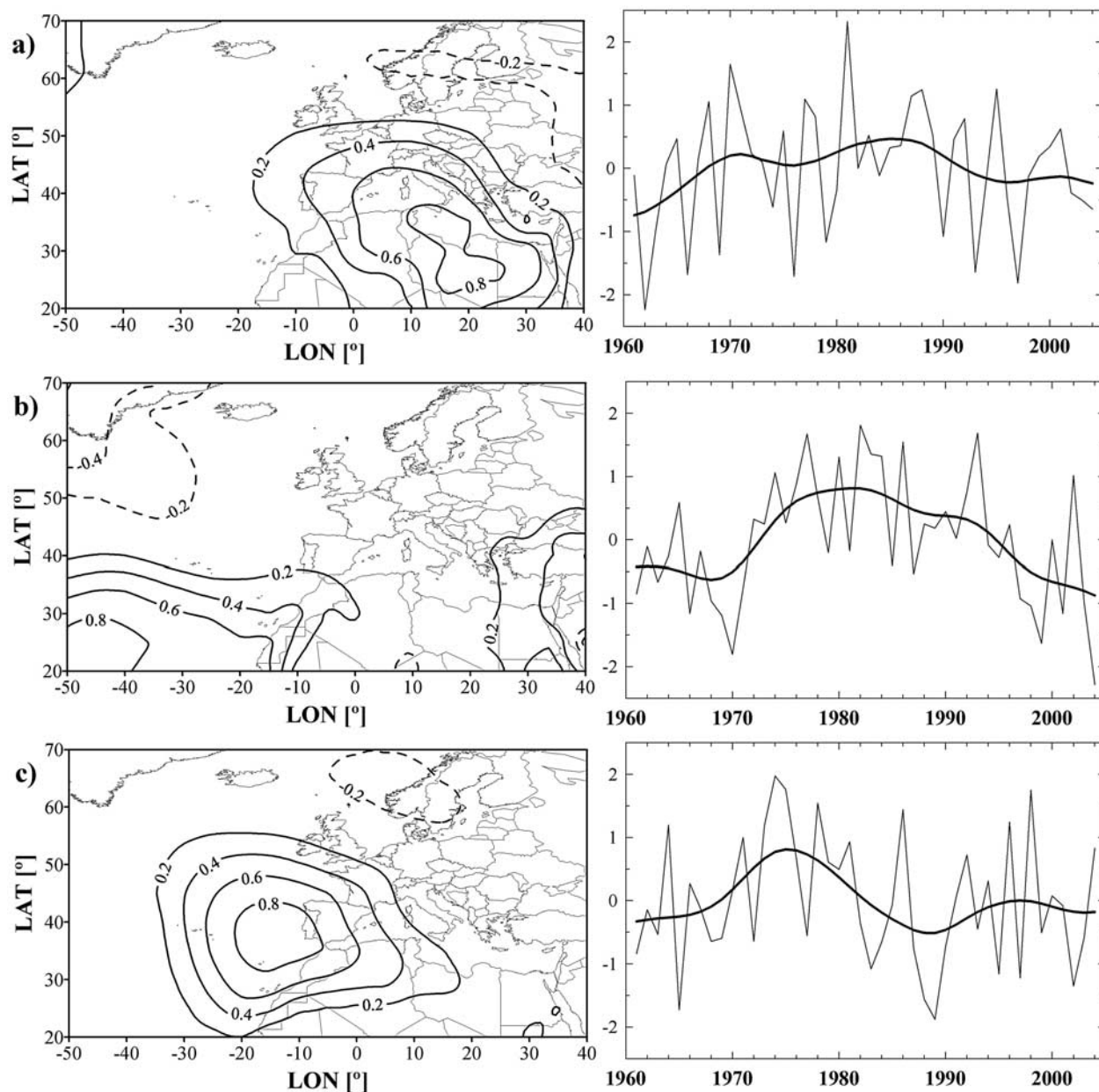


Figure 11. As in Figure 9 but in summer, and for two EOFs ((a) EOF2 and (b) EOF5).



**Figure 12.** As in Figure 9 but in autumn, and for three EOFs ((a) EOF5, (b) EOF6, and (c) EOF7).

not associated with an increase in TCC. Similar results have been demonstrated recently for northern Europe [Stjern *et al.*, 2009].

[38] The computed residual SunDu series after removal of the cloudiness-related variability, and the residual clear sky SunDu series, highlight the period of dimming from the 1960s to the early 1980s followed by a period of brightening in the most recent decades. The dimming and brightening detected here over the IP show clear resemblance with that obtained for Central Europe from more sophisticated methods and data sets [Norris and Wild, 2007] and might thus be regarded as a large-scale phenomenon. Thus, we consider that the most likely causes for the decline and subsequent recovery in the residual SunDu series and series of SunDu under clear skies are related to changes in aerosol radiative effects, corresponding with reported increases and decreases

of anthropogenic aerosols during the dimming and brightening periods, respectively. Another remarkable feature in our residual SunDu series is the strong minima reached during 1982–1984 and 1992–1993, both in the annual and seasonal series, which are likely related to aerosol emissions after the El Chichón and Pinatubo volcanic eruptions. However, to completely reject the influence of clouds in the dimming/brightening phenomena over the IP, analysis of additional cloudiness parameters besides TCC is needed (e.g., type, vertical distribution and optical thickness) [Sun *et al.*, 2007].

[39] We have also shown that interannual and decadal variability of TCC and SunDu over the IP are linked to an NAO-like pattern of SLP variability, albeit with a slight northward and eastward shift. This association is strongest during winter and weakest in summer. We have further demonstrated that TCC and SunDu variations are linked to

more regional patterns of atmospheric circulation variability identified on the basis of rotated PCA. Surprisingly, we have also detected significant correlations between particular regional atmospheric circulation patterns in spring, summer and autumn and the residual SunDu and clear sky SunDu records. These intriguing results may hint at the possibility of an impact of anthropogenic aerosols emissions on the dynamics of the atmospheric circulation at synoptic scales, and should be explored further.

[40] **Acknowledgments.** This research was supported by the Spanish Ministry of Science and Innovation (MICINN) projects NUClier (CGL2004–02325) and NUClierEX (CGL2007–62664). Arturo Sanchez-Lorenzo was granted an FPU predoctoral scholarship by the MICINN and developed part of this work while performing research at the Institute of Atmospheric Sciences and Climate, Italian National Research Council (ISAC-CNR, Bologna). The sunshine duration and cloudiness series were provided by the AEMET (Spain) and Instituto de Meteorologia (Portugal). We would like to thank the two anonymous reviewers for their useful comments. We also extend our sincere thanks to Martin Wild, Associate Editor of this special issue, for his comments and encouragement.

## References

- Abakumova, G. M., E. M. Feigelson, V. Russak, and V. V. Stadnik (1996), Evaluation of long-term changes in radiation, cloudiness, and surface temperature on the territory of the former Soviet Union, *J. Clim.*, *9*, 1319–1327, doi:10.1175/1520-0442(1996)009<1319:EOLTCT>2.0.CO;2.
- Aguilar, E., I. Auer, M. Brunet, T. C. Peterson, and J. Wieringa (2003), *Guidelines on Climate Metadata and Homogenization*, 52 pp., World Meteorol. Organ., Geneva, Switzerland.
- Alpert, P., and P. Kishcha (2008), Quantification of the effect of urbanization on solar dimming, *Geophys. Res. Lett.*, *35*, L08801, doi:10.1029/2007GL033012.
- Alpert, P., P. Kishcha, Y. J. Kaufman, and R. Schwarzbard (2005), Global dimming or local dimming?: Effect of urbanization on sunlight availability, *Geophys. Res. Lett.*, *32*, L17802, doi:10.1029/2005GL023320.
- Angell, J. K. (1990), Variation in United States cloudiness and sunshine duration between 1950 and the drought year of 1988, *J. Clim.*, *3*, 296–308, doi:10.1175/1520-0442(1990)003<0296:VIUSCA>2.0.CO;2.
- Angell, J. K., J. Korshover, and G. F. Cotton (1984), Variation in United States cloudiness and sunshine, 1950–82, *J. Clim. Appl. Meteorol.*, *23*, 752–761, doi:10.1175/1520-0450(1984)023<0752:VIUSCA>2.0.CO;2.
- Auer, I., et al. (2007), HISTALP—Historical instrumental climatological surface time series of the Greater Alpine Region, *Int. J. Climatol.*, *27*, 17–46, doi:10.1002/joc.1377.
- Barnston, A. G., and R. E. Livezey (1987), Classification, seasonality and persistence of low-frequency atmospheric circulation patterns, *Mon. Weather Rev.*, *115*, 1083–1126, doi:10.1175/1520-0493(1987)115<1083:CSAPOL>2.0.CO;2.
- Briffa, K. R., P. D. Jones, and H. Hulme (1994), Summer moisture variability across Europe, 1892–1991: An analysis based on the Palmer drought severity index, *Int. J. Climatol.*, *14*, 475–506, doi:10.1002/joc.3370140502.
- Brunetti, M., M. Maugeri, F. Monti, and T. Nanni (2006), Temperature and precipitation variability in Italy in the last two centuries from homogenised instrumental time series, *Int. J. Climatol.*, *26*, 345–381, doi:10.1002/joc.1251.
- Calbó, J., and A. Sanchez-Lorenzo (2009), Cloudiness climatology in the Iberian Peninsula from three global gridded datasets (ISCCP, CRU TS 2.1, ERA-40), *Theor. Appl. Climatol.*, doi:10.1007/s00704-008-0039-z, in press.
- Craddock, J. M. (1979), Methods of comparing annual rainfall records for climatic purposes, *Weather*, *34*, 332–346.
- Dai, A., K. Trenberth, and T. R. Kark (1999), Effects of clouds, soil moisture, precipitation, and water vapor on diurnal temperature range, *J. Clim.*, *12*, 2451–2473, doi:10.1175/1520-0442(1999)012<2451:EOCSMP>2.0.CO;2.
- Escudero, M., S. Castillo, X. Querol, A. Avila, M. Alarcón, M. M. Viana, A. Alastuey, E. Cuevas, and S. Rodríguez (2005), Wet and dry African dust episodes over eastern Spain, *J. Geophys. Res.*, *110*, D18S08, doi:10.1029/2004JD004731.
- Gilgen, H., M. Wild, and A. Ohmura (1998), Means and trends of shortwave irradiance at the surface estimated from global energy balance archive data, *J. Clim.*, *11*, 2042–2061.
- Hurrell, J. W., Y. Kushnir, M. Visbeck, and G. Ottersen (2003), An overview of the North Atlantic Oscillation, in *The North Atlantic Oscillation: Climate Significance and Environmental Impact*, *Geophys. Monogr. Ser.*, vol. 134, edited by J. W. Hurrell et al., pp. 1–35, AGU, Washington, D. C.
- Huth, R. (2006), The effect of various methodological options on the detection of leading modes of sea level pressure variability, *Tellus Ser. A*, *58*, 121–130, doi:10.1111/j.1600-0870.2006.00158.x.
- Iqbal, M. (1983), *An Introduction to Solar Radiation*, 390 pp., Academic, Toronto, Ont., Canada.
- Jones, P. A., and A. Henderson-Sellers (1992), Historical records of cloudiness and sunshine in Australia, *J. Clim.*, *5*, 260–267, doi:10.1175/1520-0442(1992)005<0260:HROCAS>2.0.CO;2.
- Jones, P. D., T. Jónsson, and D. Wheeler (1997), Extension to the North Atlantic Oscillation using early instrumental pressure observations from Gibraltar and south-west Iceland, *Int. J. Climatol.*, *17*, 1433–1450, doi:10.1002/(SICI)1097-0088(19971115)17:13<1433::AID-JOC203>3.0.CO;2-P.
- Kaiser, D. P. (2000), Decreasing cloudiness over China: An updated analysis examining additional variables, *Geophys. Res. Lett.*, *27*, 2193–2196, doi:10.1029/2000GL011358.
- Knutti, R. (2008), Why are climate models reproducing the observed global surface warming so well?, *Geophys. Res. Lett.*, *35*, L18704, doi:10.1029/2008GL034932.
- Liang, F., and X. A. Xia (2005), Long-term trends in solar radiation and the associated climatic factors over China for 1961–2000, *Ann. Geophys.*, *23*, 2425–2432.
- Liepert, B. G. (2002), Observed reductions of surface solar radiation at sites in the United States and worldwide from 1961 to 1990, *Geophys. Res. Lett.*, *29*(10), 1421, doi:10.1029/2002GL014910.
- Lolis, C. J. (2009), Winter cloudiness variability in the Mediterranean region and its connection to atmospheric circulation features, *Theor. Appl. Climatol.*, doi:10.1007/s00704-008-0046-0, in press.
- Lopez-Bustins, J. A., J. Martin-Vide, and A. Sanchez-Lorenzo (2008), Iberia winter rainfall trends bases upon changes in teleconnection and circulation patterns, *Global Planet. Change*, *63*, 171–176, doi:10.1016/j.gloplacha.2007.09.002.
- Lynch, D. K. (1996), Cirrus clouds: Their role in climate and global change, *Acta Astronaut.*, *38*, 859–863, doi:10.1016/S0094-5765(96)00098-7.
- Mace, G. G., S. Benson, and S. Kato (2006), Cloud radiative forcing at the Atmospheric Radiation Measurement Program Climate Research Facility: 2. Vertical redistribution of radiant energy by clouds, *J. Geophys. Res.*, *111*, D11S91, doi:10.1029/2005JD005922.
- Martin-Vide, J., and J. A. Lopez-Bustins (2006), The Western Mediterranean Oscillation and rainfall in the Iberian Peninsula, *Int. J. Climatol.*, *26*, 1455–1475, doi:10.1002/joc.1388.
- Maugeri, M., Z. Bagnati, M. Brunetti, and T. Nanni (2001), Trends in Italian total cloud amount, 1951–1996, *Geophys. Res. Lett.*, *28*, 4551–4554, doi:10.1029/2001GL013754.
- Norris, J. R., and M. Wild (2007), Trends in aerosol radiative effects over Europe inferred from observed cloud cover, solar “dimming,” and solar “brightening”, *J. Geophys. Res.*, *112*, D08214, doi:10.1029/2006JD007794.
- Ohmura, A., and H. Lang (1989), Secular variation of global radiation in Europe, in *IRS’88: Current Problems in Atmospheric Radiation*, edited by J. Lenoble and J.-F. Geleyn, pp. 298–301, A. Deepak, Hampton, Va.
- O’Lenic, E. A., and R. E. Livezey (1988), Practical considerations in the use of rotated principal component analysis (RPCA) in diagnostic studies of upper-air height fields, *Mon. Weather Rev.*, *116*, 1682–1689, doi:10.1175/1520-0493(1988)116<1682:PCITUO>2.0.CO;2.
- Papadimas, C. D., N. Hatzianastassiou, N. Mihalopoulos, X. Querol, and I. Vardavas (2008), Spatial and temporal variability in aerosol properties over the Mediterranean basin based on 6-year (2000–2006) MODIS data, *J. Geophys. Res.*, *113*, D11205, doi:10.1029/2007JD009189.
- Pinker, R. T., B. Zhang, and E. G. Dutton (2005), Do satellites detect trends in surface solar radiation?, *Science*, *308*, 850–854, doi:10.1126/science.1103159.
- Pozo-Vázquez, D., J. Tovar-Pescador, S. R. Gámiz-Fortis, M. J. Esteban-Parra, and Y. Castro-Diez (2004), NAO and solar radiation variability in the European North Atlantic region, *Geophys. Res. Lett.*, *31*, L05201, doi:10.1029/2003GL018502.
- Preisendorfer, R. W. (1988), *Principal Component Analysis in Meteorology and Oceanography*, 425 pp., Elsevier, Amsterdam.
- Qian, Y., D. P. Kaiser, L. R. Leung, and M. Xu (2006), More frequent cloud-free sky and less surface solar radiation in China from 1955 to 2000, *Geophys. Res. Lett.*, *33*, L01812, doi:10.1029/2005GL024586.
- Ramanathan, V., P. J. Crutzen, J. T. Kiehl, and D. Rosenfeld (2001), Aerosols, climate, and the hydrological cycle, *Science*, *294*, 2119–2124, doi:10.1126/science.1064034.
- Rimbu, N., T. Felis, G. Lohmann, and J. Pätzold (2006), Winter and summer climate patterns in the European-Middle East during recent centuries as documented in a northern Red Sea coral record, *Holocene*, *16*, 321–330, doi:10.1191/0959683606h1930rp.

- Robock, A. (2000), Volcanic eruptions and climate, *Rev. Geophys.*, *38*, 191–219, doi:10.1029/1998RG000054.
- Rosenfeld, D., U. Lohmann, G. B. Raga, C. D. O'Dowd, M. Kulmala, S. Fuzzi, A. Reissell, and M. O. Andreae (2008), Flood or drought: How do aerosols affect precipitation?, *Science*, *321*, 1309–1313, doi:10.1126/science.1160606.
- Rossow, W. B., and E. N. Dueñas (2004), The International Satellite Cloud Climatology Project (ISCCP) web site, *Bull. Am. Meteorol. Soc.*, *85*, 167–172, doi:10.1175/BAMS-85-2-167.
- Ruckstuhl, C., et al. (2008), Aerosol and cloud effects on solar brightening and the recent rapid warming, *Geophys. Res. Lett.*, *35*, L12708, doi:10.1029/2008GL034228.
- Sanchez-Lorenzo, A., M. Brunetti, J. Calbó, and J. Martin-Vide (2007), Recent spatial and temporal variability and trends of sunshine duration over the Iberian Peninsula from a homogenized data set, *J. Geophys. Res.*, *112*, D20115, doi:10.1029/2007JD008677.
- Sanchez-Lorenzo, A., J. Calbó, and J. Martin-Vide (2008a), Spatial and temporal trends in sunshine duration over Western Europe (1938–2004), *J. Clim.*, *21*, 6089–6098, doi:10.1175/2008JCLI2442.1.
- Sanchez-Lorenzo, A., J. Sigró, J. Calbó, J. Martin-Vide, M. Brunet, E. Aguilar, and M. Brunetti (2008b), Efectos de la nubosidad e insolación en las temperaturas recientes de España (in Spanish with English abstract), in *Cambio Climático Regional y sus Impactos*, *Publ. Asoc. Esp. Climatol. Ser. A*, vol. 6, edited by J. Sigró, M. Brunet, and E. Aguilar, pp. 273–283, Asoc. Esp. de Climatol., Catalonia, Spain.
- Slonosky, V. C., P. D. Jones, and T. D. Davies (2000), Variability of the surface atmospheric circulation over Europe, 1774–1995, *Int. J. Climatol.*, *20*, 1875–1897, doi:10.1002/1097-0088(200012)20:15<1875::AID-JOC593>3.0.CO;2-D.
- Solomon, S., D. Qin, M. Manning, Z. Chen, M. Marquis, K. B. Averyt, M. Tignor, and H. L. Miller (Eds.) (2007), *Climate Change 2007: The Scientific Basis: Contribution of Working Group I to the Fourth Assessment Report of the Intergovernmental Panel on Climate Change*, Cambridge Univ. Press, Cambridge, U.K.
- Stanhill, G. (2003), Through a glass brightly: Some new light on the Campbell-Stokes sunshine recorder, *Weather*, *58*, 3–11, doi:10.1256/wea.278.01.
- Stanhill, G. (2005), Global dimming: A new aspect of climate change, *Weather*, *60*, 11–14, doi:10.1256/wea.210.03.
- Stanhill, G., and S. Cohen (2001), Global dimming: A review of the evidence for a widespread and significant reduction in global radiation with discussion of its probable causes and possible agricultural consequences, *Agric. For. Meteorol.*, *107*, 255–278, doi:10.1016/S0168-1923(00)00241-0.
- Stanhill, G., and S. Cohen (2008), Solar radiation changes in Japan during the 20th century: Evidence from sunshine duration measurements, *J. Meteorol. Soc. Jpn.*, *86*, 57–76, doi:10.2151/jmsj.86.57.
- Stanhill, G., and S. Moreshet (1992), Global radiation climate changes: The world network, *Clim. Change*, *21*, 57–75, doi:10.1007/BF00143253.
- Stern, D. I. (2006), Reversal of the trend in global anthropogenic sulfur emissions, *Global Environ. Change*, *16*, 207–220, doi:10.1016/j.gloenvcha.2006.01.001.
- Stjern, C. W., J. E. Kristjánsson, and A. W. Hansen (2009), Global dimming and global brightening—An analysis of surface radiation and cloud cover data in northern Europe, *Int. J. Climatol.*, doi:10.1002/joc.1735, in press.
- Streets, D. G., Y. Wu, and M. Chin (2006), Two-decadal aerosol trends as a likely explanation of the global dimming/brightening transition, *Geophys. Res. Lett.*, *33*, L15806, doi:10.1029/2006GL026471.
- Sun, B., T. R. Karl, and D. J. Seidel (2007), Changes in cloud-ceiling heights and frequencies over the United States since the early 1950s, *J. Clim.*, *20*, 3956–3970, doi:10.1175/JCLI4213.1.
- Trenberth, K. E., and D. A. Paolino (1980), The Northern Hemisphere sea-level pressure data set: Trends, errors, and discontinuities, *Mon. Weather Rev.*, *108*, 855–872, doi:10.1175/1520-0493(1980)108<0855:TNHSLP>2.0.CO;2.
- Trenberth, K. E., et al. (2007), Observations: surface and atmospheric climate change, in *Climate Change 2007: The Physical Science Basis: Working Group I Contribution to the Fourth Assessment Report of the IPCC*, edited by S. Solomon et al., pp. 235–336, Cambridge Univ. Press, Cambridge, U.K.
- Vose, R. S., D. R. Easterling, and B. Gleason (2005), Maximum and minimum temperature trends for the globe: An update through 2004, *Geophys. Res. Lett.*, *32*, L23822, doi:10.1029/2005GL024379.
- Warren, S. G., and C. J. Hahn (2002), Clouds: Climatology, in *Encyclopedia of Atmospheric Sciences*, vol. 2, edited by J. R. Holton and J. A. Curry, pp. 476–483, Academic, San Diego, Calif.
- Warren, S. G., R. M. Eastman, and C. J. Hahn (2007), A survey of changes in cloud cover and cloud types over land from surface observations, 1971–96, *J. Clim.*, *20*, 717–738, doi:10.1175/JCLI4031.1.
- Wild, M., H. Gilgen, A. Roesch, A. Ohmura, C. L. Long, E. G. Dutton, B. Forgan, A. Kallis, V. Russak, and A. Tsvetkov (2005), From dimming to brightening: Decadal changes in solar radiation at Earth's surface, *Science*, *308*, 847–850, doi:10.1126/science.1103215.
- Wild, M., A. Ohmura, and K. Makowski (2007), Impact of global dimming and brightening on global warming, *Geophys. Res. Lett.*, *34*, L04702, doi:10.1029/2006GL028031.

M. Brunetti, Institute of Atmospheric Sciences and Climate, Italian National Research Council (ISAC-CNR), Via P.Gobetti 101, I-40129 Bologna, Italy.

J. Calbó, Group of Environmental Physics, University of Girona, Campus Motivili ESP-II, E-17071, Girona, Spain.

C. Deser, National Center for Atmospheric Research, P.O. Box 3000, Boulder, CO 80307-3000, USA.

A. Sanchez-Lorenzo, Group of Climatology, Department of Physical Geography, University of Barcelona, C/Montalegre n° 6, E-08001 Barcelona, Spain. (asanchezlorenzo@ub.edu)